

Measurement of the Electron Velocity-Field Characteristics in Germanium Using a New Technique

A. Neukermans* and G. S. Kino

*Microwave Laboratory, W. W. Hansen Laboratories of Physics, Stanford University,
Stanford, California 94305*

(Received 30 December 1971)

A new method is described that combines the Shockley-Haynes experiment with the time-of-flight technique. This technique allows absolute measurement of the velocity-field characteristic in materials too impure to be measured by the latter method. Measurements have been made with this technique on Ge, InSb, and Si, but only the Ge measurements will be reported here. It is demonstrated that negative differential mobility (NDM) occurs in the electron velocity characteristic for the $\{100\}$ direction, at a temperature as high as 200°K. At 77°K, the NDM is as large as 275 cm²/V sec. By applying uniaxial pressure, it is possible to enhance the NDM. A value of 1000 cm²/V sec is obtained at 110°K, for a pressure of 9 kbar, with electron motion in the $[11\bar{2}]$ direction, and pressure applied along the $[111]$ direction.

I. INTRODUCTION

The time-of-flight technique, first introduced by Spear¹ to measure carrier mobilities in Se, has since been successfully used to measure high-field properties of some other materials. Using this technique, Ruch and Kino² have measured the electron velocity, diffusion, and trapping coefficient of electrons in GaAs as a function of the electronic field. Several other authors³⁻⁸ have employed the technique to measure the transport properties of electrons and holes in silicon and in CdTe.⁹ Chang and Ruch¹⁰ have applied the method to the measurement of the electron velocity in Ge at low temperature.

Typically, this method uses a fully depleted back-biased p^+vn^+ structure, and carriers are created by very-fast-electron-beam injection. From the current duration, the electron (or hole) velocity can be determined, and the diffusion coefficient and trapping time can also be derived from the waveshape. (The sample length w is known.)

Meaningful measurements require a substantially uniform field in the depleted v region. The difference in field between the anode and cathode, due to space charge in the region, is given by $\Delta E = N_d ew/\epsilon$, where N_d is the net donor density, e the electron charge, and ϵ the dielectric constant. For maximum field uniformity, both N_d and w should be as small as possible to make ΔE small compared with the applied fields. N_d is limited by purity of the available materials, and w cannot be made arbitrarily small, since this reduces the pulse duration and reduces the measurement accuracy by decreasing the ratio of the pulse length to the rise time. A reasonable minimum for w is about 300 μm .

The present minimum donor concentration ob-

tainable with Ge is of the order of $3 \times 10^{11}/\text{cm}^3$; therefore, with $w = 300 \mu\text{m}$ and N_d as above we find that $\Delta E = 1000 \text{ V/cm}$. Thus, the time-of-flight method is only marginally useful for Ge, especially with uniaxial applied pressure, since the field inhomogeneity is about as large as the threshold field for negative differential mobility (NDM). In addition, as very few other semiconductors can be obtained in such a pure condition, the applicability of the method is severely limited.

In this paper we describe a modification of the time-of-flight experiment, which uses the principle of minority-carrier injection, as in the Shockley-Haynes experiment.¹¹ By using the electron-beam-injection technique, the time of measurement is decreased by almost three orders of magnitude; thus the method is far more versatile. In the classical Shockley-Haynes technique, an extrinsic semiconductor with Ohmic contacts at each end is used. A drift field is applied between these contacts. Minority carriers are injected through a separate emitting electrode at a time t_1 into the semiconductor. They move under the influence of the drift field, and at time t_2 their arrival at a separate collector electrode is observed. From the distance between the emitter and collector and the time lapse $t_2 - t_1$, the velocity of the minority carriers is obtained. In its classical configuration, this method is awkward to apply at high fields because of the large bias voltage required, and the pickup problems due to the use of a pulsed voltage supplied, and to the small time delays involved; at least one high-field adaption has been used in the past.¹²

In the experiment to be described in this paper, a sample of p -type material is used. An electron pulse is injected in the diode by passing a pulsed electron beam through a thin p^+ contact, much as in the original time-of-flight method. No separate

collector is used, but the same contact to which the drift pulse is applied is used to detect the induced-current pulse. An excess current is produced from the carriers created by the electron bombardment, and the duration of this current is again taken as the transit time. As the samples are now extrinsic, rather than semi-insulating, there is not a severe restriction on the donor density, and so a wide range of materials can be measured by this technique. In contrast to the original time-of-flight method, there is also a large Ohmic current passed through the sample when the drift field is applied. It is therefore necessary to provide suitable filtering to separate the current induced by the electron beam from the bias current. Suitable circuits for this purpose have been devised to separate out injected signals corresponding to a few millivolts amplitude from the drift pulse, corresponding to voltages of the order of several hundred volts.

With this technique, easily detectable signals can be obtained at injection levels such that the ambipolar correction required is still well within the experimental limit. Even in a material like InSb, which exhibits pronounced ambipolar effects, it turns out that the correction is not unreasonable (10–15%). Only the results obtained in Ge will be described here. The results obtained in InSb are described in the following paper.¹³

II. QUALITATIVE ANALYSIS

Consider the device shown in Fig. 1. Neglecting diffusion, the conduction current density in equilibrium is

$$j_0 = -en_0v_n + ep_0v_p \quad (1)$$

Here v_n and v_p are the electron and hole drift velocities and n_0 and p_0 are the electron and hole concentrations (usually $p_0 \gg n_0$). When an excess of electrons and holes, Δn and Δp , respectively, are introduced, there will be a change in the field in the region where the excess carriers are present, so that the velocities of the carriers will be changed by Δv_n and Δv_p , respectively. The current density is therefore

$$j = -e(n_0 + \Delta n)(v_n + \Delta v_n) + e(p_0 + \Delta p)(v_p + \Delta v_p).$$

To first order, the current density through the sample is

$$j = j_0 + e(p_0 \Delta v_p - n_0 \Delta v_n) + e(\Delta p v_p - \Delta n v_n) \quad (2)$$

The total current density $i = \epsilon(\partial E/\partial t) + j$ must be uniform through the sample, since from Maxwell's equations, in one-dimensional form,

$$\frac{\partial}{\partial x} \left(\epsilon \frac{\partial E}{\partial t} + j \right) = 0.$$

Integrating over the length of the sample, we obtain the result

$$wi = \epsilon \frac{\partial}{\partial t} \int_0^w E dx + j_0 w + e p_0 \int_0^w \Delta v_p dx - e n_0 \int_0^w \Delta v_n dx + e \int_0^w (\Delta p v_p - \Delta n v_n) dx \quad (3)$$

The second integral on the right-hand side of Eq. (3) can be written as

$$e p_0 \int_0^w \frac{\partial v_p}{\partial E} \Delta E dx \approx e p_0 \frac{\partial v_p}{\partial E} \int_0^w \Delta E dx,$$

and similarly for the term involving v_n . If we assume that the voltage across the device remains constant, then each of the first three integrals are zero. Taking $\Delta n = \Delta p$, we find that only the last term in Eq. (3) gives a contribution, so that by putting $I = I_0 + \Delta I$, where I_0 is the conduction current through the sample, and putting $\Delta Q = \int_0^w e \Delta p dx$, we find that

$$\Delta I = \Delta Q (v_p - v_n) / w.$$

As v_n and v_p are of opposite sign, it follows that

$$|\Delta I| = \Delta Q (|v_n| + |v_p|) / w \quad (4)$$

where ΔQ is the excess charge introduced per cm². It is seen that there exists a contribution both from

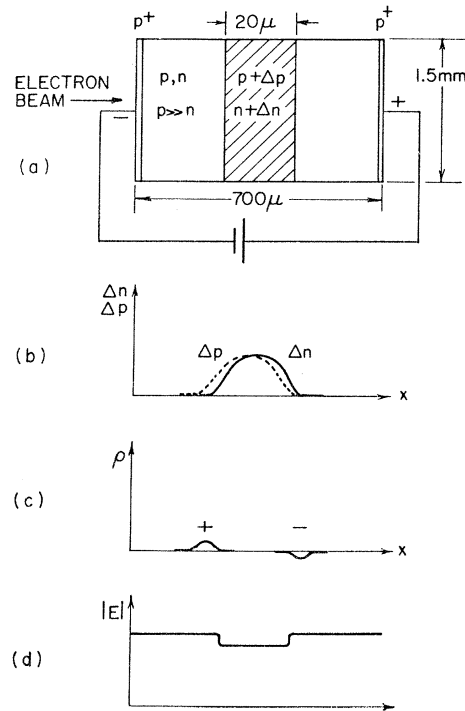


FIG. 1. Schematic illustration of the combined Shockley-Haynes and time-of-flight methods: (a) typical sample configuration; (b) excess carrier distributions; (c) space-charge distribution; (d) electric field variation.

the holes and the electrons and that the basic formula for the induced current is the same as that for the seminsulating material. The velocity with which the electrons move is of course determined by the local field they experience, as in indicated in Fig. 1(d). This is seen to be somewhat less than the average applied field because of the increased carrier density. The electric field and hence the velocity of the excess electrons is dependent upon the concentration of the injected minority carriers. The solution to this problem has, in general, been derived by Herring,¹⁴ but we will follow an approach first given by Van Roosbroek,¹⁵ and commonly called the ambipolar solution

The derivation is carried out in the Appendix. A wave equation is derived for Δn , the excess minority carrier concentration. One finds an ambipolar group velocity

$$v_{\text{am}} = - \left(v_n p \frac{\partial v_p}{\partial E} - v_p n \frac{\partial v_n}{\partial E} \right) / \left(-p \frac{\partial v_p}{\partial E} + n \frac{\partial v_n}{\partial E} \right), \quad (5)$$

and an ambipolar diffusion coefficient given by

$$D_{\text{am}} = \left(-D_n p \frac{\partial v_p}{\partial E} + D_p n \frac{\partial v_n}{\partial E} \right) / \left(-p \frac{\partial v_p}{\partial E} + n \frac{\partial v_n}{\partial E} \right). \quad (6)$$

Substitution of $-\mu_n E$ and $\mu_p E$ for v_n and v_p at low fields reduces the above quantities to the more familiar expressions

$$\mu_{\text{am}} = \frac{p - n}{p/\mu_n + n/\mu_p} \quad (7)$$

and

$$D_{\text{am}} = \frac{p + n}{p/D_n + n/D_p}. \quad (8)$$

A similar expression has been derived by Kino,¹⁶ on the basis of a carrier-wave approach; the restriction $\Delta n = \Delta p$ is not required in his treatment, but it follows from his derivation that the result is a very accurate approximation provide it is assumed that $\Delta n \ll n$ and $\Delta p \ll p$. Equation (5) can also be derived by using a carrier-wave analysis with Fourier-transform techniques. As the results obtained are based on a small-signal theory, Δn must be small compared to n , which provides certain restrictions on such experiments.

The difference between the true drift velocity of the electrons (the minority carriers) and the ambipolar velocity is

$$v_n - v_{\text{am}} = \left(n \frac{\partial v_n}{\partial E} (v_n - v_p) \right) / \left(-p \frac{\partial v_p}{\partial E} + n \frac{\partial v_n}{\partial E} \right). \quad (9)$$

It will be noted that the ambipolar velocity can be smaller than, equal to, or larger than the true electron drift velocity, depending on whether the dif-

ferential electron mobility is positive, zero, or negative. This occurs because the actual field that the excess carriers see is always smaller than the average field. To see the magnitude of these effects, consider that a 10-mV signal is desired at the sampling oscilloscope at 1500 V/cm for a sample of Ge 0.6 mm long, oriented along the [100] direction. The electron and hole velocities v_n and v_p at room temperature are 4.0×10^8 and -2.2×10^8 cm/sec, respectively, and the differential mobilities are 1750 and -1650 cm²/V sec, respectively. The effective load resistor is of the order of 33 Ω ; and therefore a 300- μ A excess current is required. The excess carrier concentration taking into account the sample dimensions is roughly 4×10^{11} electrons/cm³. For 15- Ω cm material, $p = 2.1 \times 10^{14}$ /cm³, $n = 2.7 \times 10^{12}$ /cm³, and hence, from Eq. (14), $v_n - v_{\text{am}} = 6 \times 10^4$ cm/sec. The ambipolar velocity is roughly 1.5% smaller than the true drift velocity. This correction is well within the experimental accuracy. Since the electron and hole velocities are usually known to some degree, the allowable signal can be estimated, and it is therefore possible to keep the correction small, by keeping the injection level and the observed signal small.

For this method to be accurate, it is important that a uniform field can be obtained throughout the p -type sample. This requires that the hole velocity characteristic does not show a pronounced saturation effect or NDM; otherwise there may be excess hole charge and the field may become nonuniform. For the maximum fields that have been used and (about 10 kV/cm) the typical sample dimensions (0.6–1 mm) and doping densities used, it would also seem that the space-charge injected current is still small compared to the Ohmic current.¹⁷ Probing of the samples confirmed these results, and indicated uniform fields.

Because of the nature of the experiment, there is increased electron-hole scattering, which has a first-order effect on the mobility of the electrons at least at low temperatures and low electric fields. Paige¹⁸ has experimentally demonstrated that this type of scattering can be quite important at temperatures of 77 °K or below for low fields, and his results are in good agreement with a theory of McLean and Paige¹⁹ on electron-hole scattering at zero fields. A theoretical analysis of the electron-hole scattering cross section at high fields does not yet exist, and is not an easy problem. We have not made any corrections to our data to take this effect into account. This would appear to be reasonable when it is considered that the electron-hole scattering, which is of a Coulomb nature, varies at $1/v_{\text{th}}^3$, where v_{th} is the thermal velocity of the carrier. Therefore when electron heating takes place, the scattering becomes negligible. Our experimental observations are also in good

agreement, as far as the magnitude of the velocity is concerned, with those of Chang and Ruch,¹⁰ who used the time-of-flight technique in a semiinsulating material where electron-hole scattering is virtually nonexistent.

The method described here may be compared to that used in the Shockley-Haynes experiment. Our technique uses no collector or emitter and has a geometrically well-defined path length for the electrons, the surface recombination is negligible, and materials that have a much shorter lifetime and trapping time can be used. Typically, the transit time is more than three orders of magnitude smaller than in the classical configuration, there are few pickup problems, and it is capable of measuring the velocity at much higher fields. On the other hand, it does require very good Ohmic contacts, which are also very thin ($< 1 \mu\text{m}$). These are not always easy to make by conventional means, although the advent of ion implantation should considerably ease this difficulty. Diffusion measurements are much harder to make with this new technique than with the Shockley-Haynes technique. Experimentally it is observed that the fall time of the signal is very sensitive to the amount of injection, more than can be accounted for by ambipolar effects. This is probably due to the fact that the minority carriers arriving at the anode are re-received at a contact that is mainly constructed to inject holes.²⁰ These difficulties coupled with the possibility of electron-hole scattering lead us to conclude that, when possible, the time-of-flight method used with the semiinsulating material should be preferred to this technique, although with many materials it is not possible to do this.

III. EXPERIMENTAL SETUP AND SAMPLE PREPARATION

The experimental setup consists of an electron gun and deflection system, a vacuum system, a bias and filter arrangement, and a sampling oscilloscope. The sample is biased and simultaneously bombarded by high-energy electrons (10–12 kV) from a cathode-ray gun. The electron beam is swept laterally across the sample aperture at very high speed by applying a fast ramp voltage to a pair of deflection plates. These high-energy electrons come into equilibrium with the lattice and create electron-hole pairs in the process. Typically, the energy required to create an electron-hole pair by this process is 2.9 eV in Ge,²¹ and penetration depth is of the order of $1 \mu\text{m}$. The multiplication process occurs very fast (in a time smaller than 100 psec) and this time lapse is insignificant in our measurement. The excess current is filtered out from the bias voltage and is displayed on a sampling oscilloscope (HP 185B).

Because of the use of an electron beam, the sample must be placed in vacuum. External cooling

baths are provided to bring the sample to the desired temperature. By the use of a Vacion pump and a getter pump, a pressure of 1×10^{-8} Torr was routinely achieved in the system. It was found that operation at these pressures significantly improved the lifetime of the oxide-coated cathode. Since the vacuum is broken every time a new sample is loaded, the cathode is somewhat contaminated by exposure to air. These effects were minimized by letting the system up to an over pressure of nitrogen, and by keeping the 6.3-V filament of the cathode heated with about 2 V. This way it was found that the system could be opened well over 30 times before cathode failure.

A cathode-ray tube from an HP 195 oscilloscope was used as an electron gun, and a 210-V 12-nsec-rise-time pulse from an HP 214 pulse generator was applied to the first set of deflection plates. A lateral-beam velocity of 5.15×10^8 cm/sec was obtained giving an injection time of 195 psec across a 1-mm aperture. The rise time of the pulse applied to the deflection pulse was decreased by a factor of 4 from that obtained directly with the use of an HP 214 pulser, by using a snap varactor. With this technique it was possible to obtain an effective electron injection time of about 50 psec.

The deflection pulse is triggered by the bias generator which supplies the drift field across the sample. Repetition rates from 20 to 60 cycles/sec were used, depending upon the amount of bias voltage applied and the resistivity of the samples. Because of the low repetition rate and because the samples are rather thin and flat, and in immediate contact with metal in the back and the front, the temperature rise is not a severe problem.

The major experimental difficulty that arises with this technique is the separation between the large bias voltage, which can be as much as 800 V, and the induced signals which are of the order of 10 to 20 mV. Since the sampling oscilloscope can only tolerate a few volts, a filter must be designed so as to reduce the bias voltage to a transient of a few volts at the scope, while not disturbing the desired signal. Various schemes were tried; however, by far the best results were obtained with the system illustrated in Fig. 2. The filter consists in essence of two coaxial shorted lines and a coaxial capacitor. The length of the lines is variable, and their length is chosen such that the round-trip time of a signal on the line is slightly in excess of the duration of the excess current that is created by the electron bombardment. Thus for the induced pulse, these lines present an impedance of 50Ω . The line in front of the filter serves to delay the reflection that occurs at the first shorted line. The second line is terminated by a $10\text{-}\Omega$ load to increase the decay of the bias transients. The equivalent circuit at low frequen-

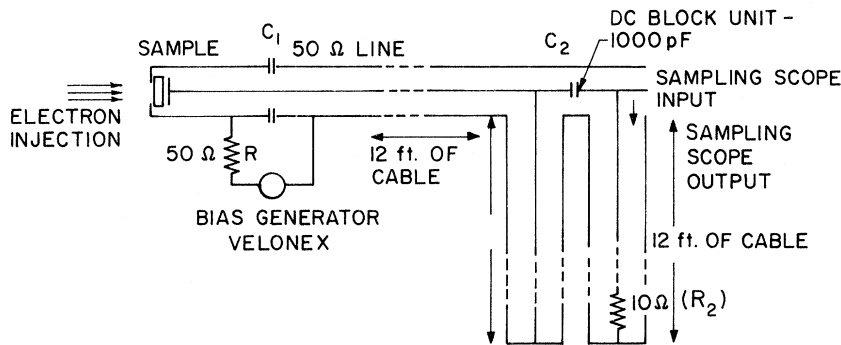


FIG. 2. Filter and bias schematic. At high bias voltages, all cable lengths are reduced to 6 ft. Various values of C_1 are chosen depending on the sample resistivity.

cies is illustrated in Fig. 3(a) and is in effect a high-pass filter. At low frequencies the shorted lines merely act as small inductances. For short time intervals, shorter than the round-trip time of an electromagnetic signal on the shorted lines, a different equivalent circuit applies, as illustrated in Fig. 3(b). The excess current is represented by a current generator and is loaded by the sample and the line. R_s is to be considered the dynamic resistance of the sample at the time when the injection occurs and at high fields is typically 4–5 times higher than at low fields. A voltage pulse of magnitude

$$R_s / (R_s + Z_0) \Delta I$$

is sent down the 50- Ω line. Since at the end of the line the impedance is roughly 25 Ω , the reflection coefficient is

$$\Gamma = (Z_L - Z_0) / (Z_L + Z_0) = -\frac{1}{3} . \quad (10)$$

The observed voltage on the scope is

$$\Delta V = \frac{2}{3} [R_s / (R_s + Z_0)] \Delta I . \quad (11)$$

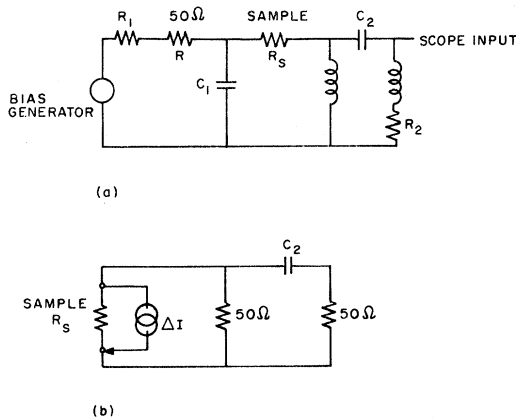


FIG. 3. (a) Equivalent circuit at low frequency. (b) Equivalent circuit for disturbances shorter than the round-trip time on the shorted lines.

Due to the capacitance C_2 , there will of course be a slight drop in voltage with time, but the resultant time constant is of the order of 75 nsec, and the voltage drop is small since the pulse duration is 10–15 nsec at most. A typical signal observed on the sampling scope is illustrated in Fig. 4. The transit time is taken to be the pulse width at half-height.

The samples were all made from high-purity p -type germanium, with resistivities of 15 and 25 Ω cm at room temperature. Appropriately oriented crystals were lapped and etched to the desired thickness. Contacts were made to the samples by diffusing 0.5–0.7 μm of Ga or In in a closed evacuated quartz tube. After diffusion, 500 \AA of In is evaporated on one side, and about 7000 \AA on the other sides. As In does not wet the surface of Ge it is important to keep the alloying temperature close to the eutectic temperature of In-Ge (156 $^\circ\text{C}$) since otherwise balling up of the indium tends to occur. The samples are then cut on the wire saw to dimensions of roughly 1.5 \times 1.5 \times 0.7 mm for the samples without pressure and 1 \times 1 \times 1 mm for those used in pressure experiments. The broad sample faces were then covered with Mylar

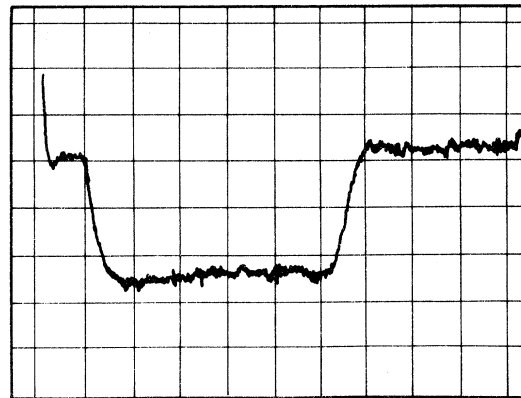


FIG. 4. Typical retrieved excess current pulse. The velocity is determined from the half-height pulse width. Horizontal scale: 2 nsec/cm; vertical scale: 10 mV/cm.

tape and the sides reetched in CP_4 and H_2O_2 to improve the breakdown voltage. Samples made this way could withstand fields up to about 20 kV/cm without injection. For the pressure experiments, the [111] faces are lapped flat and parallel to a very high degree; since no etching could be performed after the polishing operation, surface breakdown would usually occur at 8–9 kV/cm. Orientation of the pressure samples was correct within 2° .

Pressure was applied to the samples by means of the spring mechanism illustrated in Fig. 5. This design has the advantage that it can be fitted to the end of a 50- Ω line, without introducing a major disturbance, and yet has good thermal conductivity at low temperatures. Its dimensions had to be small to fit the vacuum chamber (1.2 in. diam \times 0.5 in.), but it could deliver up to 200 kg of force without exceeding the elastic limit. The sample is placed between highly polished sapphire jaws, and pressure is applied by means of a screw. The transverse deflection is measured and provides an indication of the applied pressure. Accuracy of the pressure reading was within 2 kg. With careful mounting and polishing of the germanium crystals it was possible to obtain pressures of the order of 10 kbar without fracture. This is about a factor of 2–3 lower than can be achieved in the usual uni-

axial pressure devices, which are, however, several orders of magnitude larger in volume. Since the diameter of the spring is measured at room temperature, there will be a slight increase in pressure when the temperature is decreased. At 110 $^\circ\text{K}$ and 9 kbar, this correction is of the order of 5%. Due to the radiation from the walls, and the fairly long thermal path, the sample would not reach the temperature of the external cooling path. With liquid nitrogen, the equilibrium temperature was 110 $^\circ\text{K}$, and with dry ice and alcohol it was 226 $^\circ\text{K}$.

IV. EXPERIMENTAL RESULTS IN UNSTRESSED Ge

High-purity p -type samples of 15- and 25- Ω cm resistivity were used. Although no difference was found in the high-field properties of these materials, the low-field mobility (at 100 V/cm) was found to be different and in agreement with what would be expected from ambipolar theory. In the 15- Ω cm material ($p = 2.1 \times 10^{14}/\text{cm}^3$, $n = 2.7 \times 10^{12}/\text{cm}^3$) the measured transit-time mobility was found to be 3900 $\text{cm}^2/\text{V sec}$, and for the 25- Ω cm material, 3420 $\text{cm}^2/\text{V sec}$ ($p = 12 \times 10^{14}/\text{cm}^3$, $n = 4.8 \times 10^{12}/\text{cm}^3$). The calculated mobilities are, respectively, 3850 and 3500 $\text{cm}^2/\text{V sec}$. The results of the measurements at room temperature for various crystallographic directions are illustrated in Fig. 6. The results illustrated are the average of four samples, two of each resistivity with corrections made for ambipolar effects. The [11 $\bar{2}$] direction has also been measured, but is not indicated; the measured values are slightly lower than those for the [110] direction.

It is seen that substantial anisotropy is present at high fields. The saturation velocity in the [100] direction exceeds that in the [111] direction by as much as 20%. The anisotropy is caused by the many-valley band structure of Ge; a large electric field causes differential heating and repopulation of the various [111] valleys, and this in turn causes the field and the current to be noncollinear, a phenomenon known as the Sasaki²² effect. However, in the symmetry directions of the crystal, j and E must still be aligned (the [110] direction presents a peculiar situation, however, since the field direction is threefold degenerate²³). In Ge, with the main valleys in the [111] direction, the current should be largest in the [100] direction where all valleys are symmetric with respect to the current direction, and minimum in the [111] direction. One would expect that the anisotropy should eventually decrease at very high fields since the electron temperature in all valleys is high enough so that sufficient backscattering occurs to equalize the population in all valleys. The qualitative aspects of this theory have been borne out in experiments. Early measurements by Nathan²⁴ and Barrie and

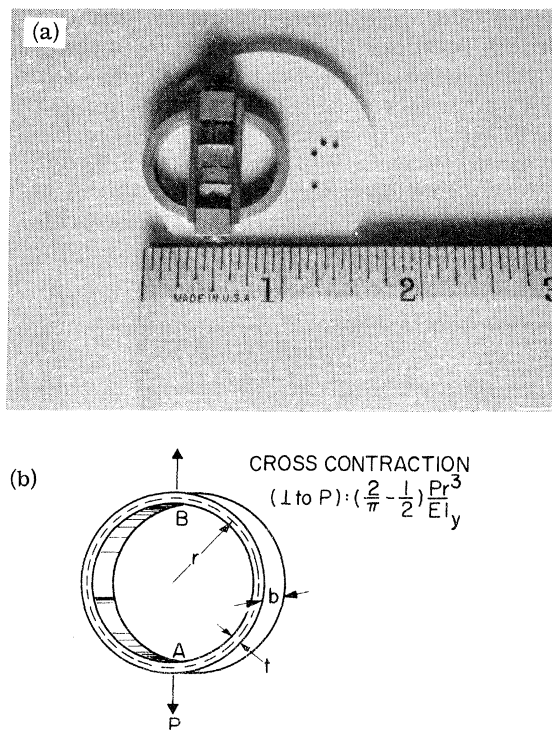


FIG. 5. (a) Photograph of the pressure mechanism. (b) Basic spring mechanism.

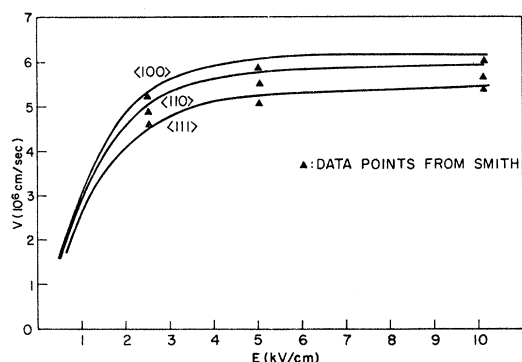


FIG. 6. Measured electron velocity vs field in the [100], [110], and [111] directions taken at $T=300^\circ\text{K}$.

Burgess²⁵ did not show appreciable anisotropy at room temperature. More recent microwave measurements by Dienys and Pozehla²⁶ indicate that the conductivity in the [100] direction exceeds the conductivity in the [111] direction at fields of about 3 kV/cm by about 15%. This anisotropy is also borne out by the more recent measurements of Smith²⁷; some data points from Smith are indicated in Fig. 6. However, in contrast to his measurement, we do observe a complete saturation of the electron velocity characteristic in the [100] direction for fields from 5–10 kV/cm. Almost complete saturation is obtained for the [110] direction and a positive differential mobility of the order of 50 cm²/V sec is maintained at the highest field in the [111] direction. The measured anisotropy is of the order of 20% in the region 3–4 kV/cm.

The experimental results at 200 °K are given in Fig. 7. The anisotropy is seen to be substantially enhanced and reaches values of the order of 30%. In the [111] and [11 $\bar{2}$] directions, a slight positive mobility exists, whereas in the [110] direction complete saturation occurs. We have also observed for the first time that NDM occurs in the [100] direction at 200 °K. An early calculation by Fawcett and Paige²⁸ for the [100] direction gives an NDM at 150 °K of 100 cm²/V sec, with a threshold of about 5 kV/cm. Our experimentally observed values are 80 cm²/V sec and 6 kV/cm at 200 °K.

The data taken at 80 °K are given in Fig. 8. The velocity difference at high fields between the [100] and [111] directions is now approximately 50% at fields of the order of 2 kV/cm. Rather pronounced NDM (275 cm²/V sec) is observed in the [100] direction, a very slight NDM (40–50 cm²/V sec) exists in the [110] direction, and almost complete saturation exists for the [11 $\bar{2}$] and [111] directions. The time-of-flight measurements of Chang and Ruch¹⁰ in comparison do not demonstrate such a large NDM; for the [100] direction, they quote a value of 80 cm²/V sec extending in a region from 2.2 to 4.3 kV/cm. However, as already pointed out, be-

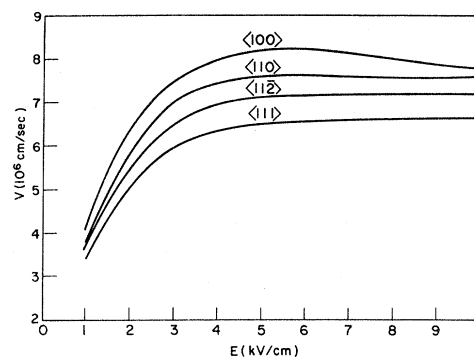


FIG. 7. Electron velocity vs field in the [100], [110], [11 $\bar{2}$], and [111] directions at $T=200^\circ\text{K}$.

cause the field in the purest material obtainable is nonuniform, the time-of-flight technique is not an optimum one for germanium. As far as the magnitude of the velocities is concerned, the agreement of both methods is rather good, at least in the [100] and [110] directions. The maximum velocities in the [100] and [110] directions obtained by Chang²⁹ are 1.18×10^7 and 1.15×10^7 cm/sec vs 1.12×10^7 and 1.10×10^7 cm/sec observed with our technique. Both measurements have in common that they yield velocities that are 20% lower than those that are measured by microwave or very fast measurements of conduction current. They are in better agreement with earlier reported saturation values, but still incapable of detecting NDM.

Quite good agreement, but probably fortuitous, can be obtained with the calculations of Fawcett and Paige²⁸ for the [100] direction already discussed if a scale factor of 0.76 is applied to their calculations. The latter is introduced to make the calculated saturation velocity at room-temperature velocity agree with the observed value. In a latter and more rigorous calculation,³⁰ they used the Monte Carlo technique, so that no assumptions concerning the distribution function have to be made.

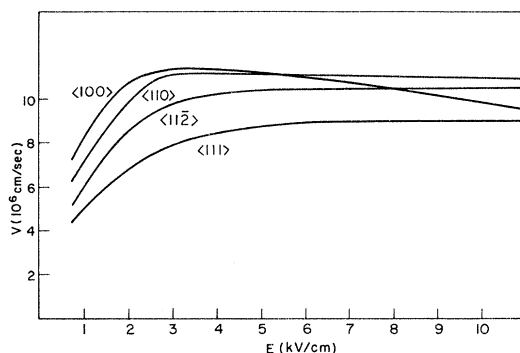


FIG. 8. Electron velocity vs field in the [100], [110], [11 $\bar{2}$], and [111] directions at $T=80^\circ\text{K}$.

This model gives saturation at 150 °K and a smaller NDM of $160 \text{ cm}^2/\text{V sec}$ at 77 °K. Although the model should be more accurate, the discrepancy at 300 °K between the calculated saturation velocity of $8 \times 10^6 \text{ cm/sec}$ in the [100] direction and the observed velocity of $6.1 \times 10^6 \text{ cm/sec}$ is still substantial. In a more recent and as yet unpublished calculation,³¹ they have obtained a better fit between the Monte Carlo method and the room-temperature saturation velocity. The modification was done to bring the model in better agreement with recent observations from small-field hydrostatic-pressure measurements. As a general result, the maximum velocities are lowered, and the NDM is increased and continues to exist even at 150 °K. In addition, Baynham,³² using microwave-absorption techniques, has observed an NDM as large as $300 \text{ cm}^2/\text{V sec}$ in the [100] direction. Thus it now seems possible that the NDM may have been previously underestimated.

Since the discovery of microwave oscillations at 77 °K in Ge by McGroddy and Nathan,³³ various other mechanisms in addition to interband transfer effects have been suggested, such as nonparabolicity of the [111] band at high energies, scattering to impurity states connected with the [100] minimum, and the fact that equipartition is not completely valid for the acoustic phonons involved in the scattering of high-energy electrons. However, most of these mechanisms only begin to have considerable effect at energies where transfer is already important, and usually give only very weak NDM. In view of our results, the intervalley transfer would seem to be the main factor. The NDM in the [110] direction is found to be much less than the NDM in the [100] direction, as predicted from intervalley transfer.

V. EXPERIMENTAL RESULTS IN STRESSED Ge

All measurements, with the samples under uniaxial pressure, were taken with pressure applied

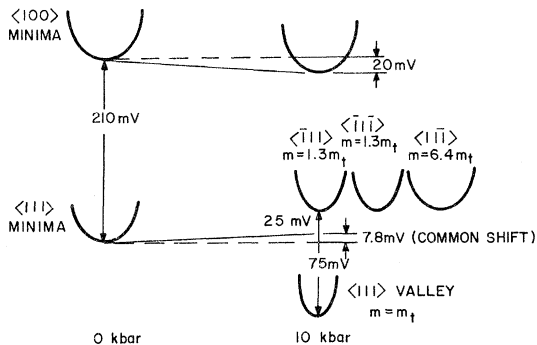


FIG. 9. Energy-minima separation as a function of uniaxial pressure in the [111] direction. The equivalent masses are for current in the [112] direction.

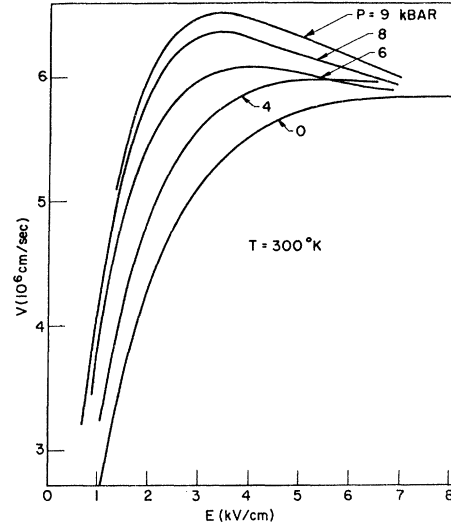


FIG. 10. Velocity-field characteristic as a function of pressure at 300 °K. The current is in the [112] direction and the uniaxial pressure in the [111] direction.

in the [111] direction and electron motion in the [112] direction. *p*-type germanium itself can exhibit instabilities at low temperature, because of hole-transfer effects, with the pressure and applied electric field collinear in the [111] direction.³⁴ No effects of NDM or very pronounced saturation of the hole characteristic were observed in the experimental configuration where the pressure and field are perpendicular. The potential was, therefore, assumed to be uniform, but the probe tests could not be performed in this arrangement. The presence of uniaxial pressure in the [111] direction removes the degeneracy of the four [111] valleys, whereas the [100] set remains degenerate. The splitting to be expected for this configuration is as illustrated in Fig. 9. The [111] valley is lowered by about 100 mV for a pressure of 10 kbar with respect to the three other valleys. These remain degenerate, as is required by symmetry. It is seen that the ratio of the conduction masses is such that negative differential conductivity can occur, as was first demonstrated by Smith.³⁵ The splitting between the valleys is given by $\delta E = \frac{4}{3} \Xi_u p S_{44}$, whereas the common shift is given by $-p(S_{11} + S_{12}) \times (\Xi_d + \frac{1}{3} \Xi_u)$. Here Ξ_d and Ξ_u are the deformation potentials (-7.1 and 15.8 eV, respectively) and S_{11} , S_{12} , and S_{44} are the elastic-compliance coefficients ($S_{11} = 9.51 \times 10^{-7} \text{ cm}^2/\text{kg}$, $S_{12} = -2.59 \times 10^{-7} \text{ cm}^2/\text{kg}$, $S_{44} = 1.457 \times 10^{-6} \text{ cm}^2/\text{kg}$).

The data taken at 300 °K for various pressures are illustrated in Fig. 10. The curves drawn are again the average for four samples, two with a room-temperature resistivity of $25 \text{ } \Omega \text{ cm}$ and two of $15 \text{ } \Omega \text{ cm}$. Up to 4 kbar no NDM is present, but the velocity at a given field is increased. With

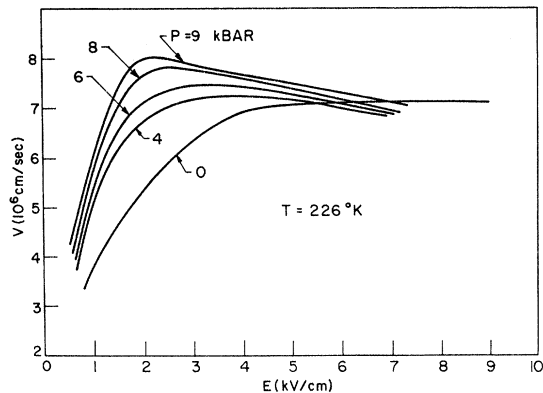


FIG. 11. Velocity-field characteristic as a function of pressure at 226 °K. The current is in the $[11\bar{2}]$ direction and the uniaxial pressure in the $[111]$ direction.

increasing pressure, NDM sets in and the velocity keeps increasing. At 9 kbar, the NDM is about $140 \text{ cm}^2/\text{V sec}$, and the velocity at 1 kV/cm has almost been doubled with respect to zero pressure. The threshold for instability is seen to decrease with pressure. Decreasing the temperature increases these effects as seen in Figs. 11 and 12; the thresholds are lowered and the NDM increases. At 9 kbar and 226 and 110 °K, the NDM near the threshold is, respectively, 250 and $1000 \text{ cm}^2/\text{V sec}$. The low-field mobility is, of course, significantly increased since the effective conductivity mass is now m_t , for at large pressures only the lower-mass minimum is substantially populated. The maximum velocity at 110 °K is $1.25 \times 10^7 \text{ cm/sec}$ up 30% from its zero-pressure value. Measured domain velocities in an n -type material with this pressure at 77 °K were about $1.4 \times 10^7 \text{ cm/sec}$.

The threshold for oscillations, as derived by Smith *et al.*,³⁴ are compared with our data in Fig. 13. The agreement is not very good, and larger thresholds are obtained by our method. However,

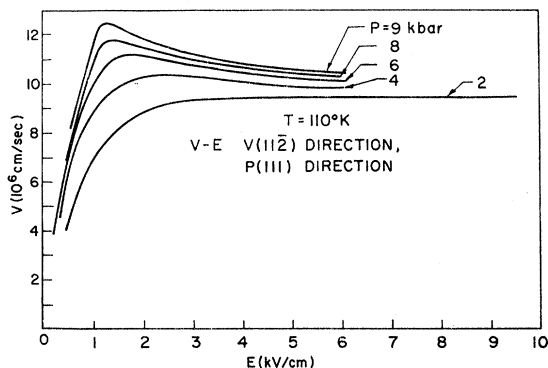


FIG. 12. Velocity-field characteristic as a function of pressure at 110 °K.

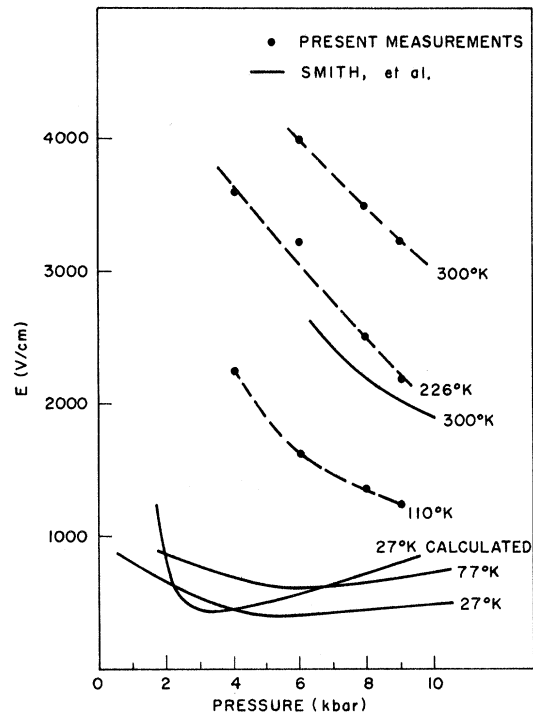


FIG. 13. Threshold vs pressure. The current is in the $[11\bar{2}]$ direction and the uniaxial pressure in the $[111]$ direction.

thresholds obtained by the observation of domain oscillations usually give values that are too low, due to local high fields at the contacts. In addition, because of the nature of the NDM here, it is possible that a local-strain concentration can create a region where NDM exists, long before the bulk of the material is sufficiently strained to obtain threshold. Such phenomena will affect threshold measurements very markedly, but will not affect our results, since the total transit time is more closely dependent on the average pressure rather than the peak pressure.

In general, the threshold dependence does not agree with the model of Butcher, Fawcett, and Hilsum³⁶ for GaAs, which predicts that a threshold minimum will occur at an energy separation kT , where T is the lattice temperature. Our data do not show any threshold minimum at energy separations several times kT , and the minima from Smith's observations also occur at much higher energies than kT . Smith and McGroddy³⁷ have performed a McCumber-Chynoweth-type calculation³⁸ and obtained semiquantitative agreement with their experiments. However, the calculated thresholds are in most cases markedly higher than the observed ones. A calculation, using the Monte Carlo method, has not yet been applied to deal with the effect of pressure. Such a calculation and compar-

ison with the experimental results could give substantial insight into the transfer process, since the energy separations, scattering coefficients, and effective masses are fairly well known for Ge.

ACKNOWLEDGMENT

The authors would like to thank Dr. W. Bond who designed the simple and elegant pressure mechanism used in our experiments.

APPENDIX A: AMBIPOLAR EQUATIONS WITH FIELD-DEPENDENT MOBILITY

The derivation is similar to the one given by Van Roosbroel, but the field dependence of the mobility will be taken into account. We will consider that space charge holds everywhere, hence $\Delta n = \Delta p$. The partial derivatives of n or Δn are then equal to these for p and Δp . The electron and hole current densities are

$$j_n = -e \left(n v_n - D_p \frac{\partial n}{\partial x} \right) \quad (\text{A1})$$

and

$$j_p = e \left(p v_p - D_p \frac{\partial p}{\partial x} \right). \quad (\text{A2})$$

From continuity, neglecting recombination, and trapping, we obtain the result

$$\begin{aligned} \frac{\partial n}{\partial t} &= \frac{1}{e} \frac{\partial j_n}{\partial x} = - \frac{\partial}{\partial x} \left(n v_n - D_n \frac{\partial n}{\partial x} \right) \\ &= -v_n \frac{\partial n}{\partial x} - n \frac{\partial v_n}{\partial E} \frac{\partial E}{\partial x} + D_n \frac{\partial^2 n}{\partial x^2} \end{aligned} \quad (\text{A3})$$

and

$$\frac{\partial p}{\partial t} = -v_p \frac{\partial p}{\partial x} - p \frac{\partial v_p}{\partial E} \frac{\partial E}{\partial x} + D_p \frac{\partial^2 p}{\partial x^2}. \quad (\text{A4})$$

Eliminating the terms in $\partial E / \partial x$, and using the relation $\partial n / \partial t = \partial \Delta n / \partial t$, we find that

$$\begin{aligned} \frac{\partial \Delta n}{\partial t} &\left(-p \frac{\partial v_p}{\partial E} + n \frac{\partial v_n}{\partial E} \right) \\ &= \frac{\partial \Delta n}{\partial x} \left(v_p p \frac{\partial v_n}{\partial E} - v_p n \frac{\partial v_n}{\partial E} \right) \\ &\quad + \frac{\partial^2 \Delta n}{\partial x^2} \left(-D_n p \frac{\partial v_p}{\partial E} + D_p n \frac{\partial v_n}{\partial E} \right). \end{aligned} \quad (\text{A5})$$

This is seen to be a wave equation for Δn , with an ambipolar group velocity

$$V_{\text{am}} = - \left(v_n p \frac{\partial v_p}{\partial E} - v_p n \frac{\partial v_n}{\partial E} \right) / \left(-p \frac{\partial v_p}{\partial E} + n \frac{\partial v_n}{\partial E} \right) \quad (\text{A6})$$

and an ambipolar diffusion coefficient given by

$$D_{\text{am}} = \left(-D_n p \frac{\partial v_p}{\partial E} + D_p n \frac{\partial v_n}{\partial E} \right) / \left(-p \frac{\partial v_p}{\partial E} + n \frac{\partial v_n}{\partial E} \right). \quad (\text{A7})$$

*Now at Xerox Research Laboratory, Webster, N. Y. 14603.

¹W. E. Spear, Proc. Phys. Soc. **78**, 826 (1960).

²J. G. Ruch and G. S. Kino, Appl. Phys. Lett. **10**, 40 (1967).

³C. B. Norris and J. F. Gibbons, IEEE Trans. Electr. Dev. **ED-14**, 38 (1967).

⁴T. W. Sigmon and J. F. Gibbons, Appl. Phys. Lett. **15**, 320 (1969).

⁵H. R. Zulliger, C. B. Norris, T. W. Sigmon, and R. H. Pehl, Nucl. Instrum. Methods **70**, 125 (1969).

⁶A. Alberigi Quaranta, F. Cipolla, and M. Martini, Phys. Lett. **17**, 102 (1965).

⁷A. Alberigi Quaranta, G. Casadei, M. Martini, G. Ottaviani, and G. Zanarini, Nucl. Instrum. Methods **35**, 93 (1961).

⁸A. Alberigi Quaranta, M. Martini, G. Ottaviani, G. Redaelli, and G. Zanarini, Solid State Electron. **11**, 685 (1968).

⁹C. Canali, G. Ottaviani, M. Martini, and K. Zaino, Appl. Phys. Lett. **19**, 51 (1971).

¹⁰D. M. Chang and J. G. Ruch, Appl. Phys. Lett. **12**, 111 (1968).

¹¹J. R. Haynes and W. Shockley, Phys. Rev. **75**, 691 (1949).

¹²A. F. Gibson and J. W. Granville, J. Electron. **2**, 259 (1956).

¹³A. Neukermans and G. S. Kino, following paper, Phys. Rev. **7**, 2703 (1973).

¹⁴C. Herring, Bell System Tech. J. **28**, 401 (1949).

¹⁵W. Van Roosbroek, Phys. Rev. **91**, 282 (1953).

¹⁶G. Kino, IEEE Trans. Electr. Dev. **ED-17**, 178 (1970).

¹⁷T. E. Seidel and D. I. Scharfetter, J. Phys. Chem. **28**, 2563 (1967).

¹⁸E. G. Paige, J. Phys. Chem. Solids **16**, 207 (1960).

¹⁹T. P. McLean and E. G. Paige, J. Phys. Chem. Solids **16**, 220 (1960).

²⁰J. B. Arthur, A. F. Gibson, and J. B. Gunn, Proc. Phys. Soc. Lond. B **69**, 697 (1956).

²¹G. Bertolini and A. Coche, *Semiconductor Detectors* (American Elsevier, New York, 1968).

²²W. Sasaki and M. Shibuya, J. Phys. Soc. Japan **11**, 1202 (1956).

²³H. G. Reik and H. Risken, Phys. Rev. **124**, 777 (1962); Phys. Rev. **126**, 1737 (1962).

²⁴M. I. Nathan, Phys. Rev. **130**, 2201 (1963).

²⁵R. Barrie and R. Burgess, Can. J. Phys. **40**, 1056 (1962).

²⁶V. Dienys and J. Pozebla, Phys. Status Solidi **17**, 769 (1966).

²⁷J. E. Smith, Phys. Rev. **178**, 1364 (1969).

²⁸W. Fawcett and E. G. Paige, Electron. Lett. **3**, 505 (1967).

²⁹D. M. Chang, Ph.D. thesis (Stanford University, 1969) (unpublished).

³⁰E. G. Paige, IBM J. Res. Develop. **13**, 562 (1969).

³¹E. G. Paige (private communication).

³²C. Baynham (private communication).

³³J. C. McGroddy and M. I. Nathan, IBM J. Res. Develop. **11**, 337 (1967).

³⁴J. E. Smith, J. C. McGroddy, and M. I. Nathan, Phys. Rev. **186**, 727 (1969).

³⁵J. E. Smith, Appl. Phys. Lett. **12**, 233 (1968).

³⁶P. N. Butcher, W. Fawcett, and C. Hilsum, IEEE Trans. Electron. Dev. **ED-13**, 192 (1966).

³⁷J. E. Smith, J. C. McGroddy, and M. I. Nathan, in *Proceedings of the Ninth International Conference on the Physics of Semiconductors*, edited by S. M. Ryvkin (Nauka, Leningrad, 1968), p. 950.

³⁸D. E. McCumber and A. G. Chynoweth, IEEE Trans. Electron Dev. **ED-13**, 4 (1966).

Absolute Measurement of the Electron Velocity-Field Characteristic of InSb

A. Neukermans* and G. S. Kino

Microwave Laboratory, W. W. Hansen Laboratories of Physics, Stanford University, Stanford, California 94305

(Received 30 December 1971)

Absolute measurements of the electron velocity in InSb at low and high fields have been made, using the combined Shockley-Haynes and time-of-flight technique. Low-field mobilities of 7×10^5 cm/V sec are reported and negative differential mobility is observed at high fields. By comparing the experimental results with numerical solutions of the ambipolar equations, it is demonstrated that the ambipolar errors are of the order of 10–15%. The experimental results are in good agreement with previous low-field measurements and agree over the whole range with the recent Monte Carlo calculations of Fawcett and Ruch.

I. INTRODUCTION

Drift mobilities of electrons in InSb have in the past been measured by making use of simultaneous pulse conductivity and Hall measurements.^{1,2} The number of carriers is determined from the Hall measurement, and hence the mobility can be determined from the conduction current. Absolute measurements like the Shockley-Haynes experiment fail because of the very fast trapping that takes place.³ By making use of an electron-beam injection technique, which we have employed previously to measure electron mobility in *p*-type Ge,⁴ we have succeeded in making absolute measurements of the velocity-field characteristics in InSb. This method combines the Shockley-Haynes technique with the time-of-flight method.

Transit times of the electrons in the sample are of the same order or less than the trapping times, and therefore the trapping does not limit the measurement as much as in other techniques. Absolute measurements were obtained in high-resistivity material; in more impure material the trapping is, however, too pronounced, and excessive injection of electrons is required to obtain a waveform that can be used for a measurement. It is demonstrated, however, by solving the nonlinear ambipolar equations numerically, that in general the ambipolar correction is substantially smaller than what would be expected from the linear theory.

Initial experiments were limited to fairly low fields (100–200 V/cm). The observation of Gunn

oscillations by Smith *et al.*⁵ in unstressed InSb, stimulated interest in the high-field region ($E > 400$ V/cm). The existence of negative differential mobility (NDM) was confirmed experimentally, as reported earlier.⁶ For both the high- and low-fields regions, there exists good agreement between the Monte Carlo calculations of Fawcett and Ruch⁷ and our results.

II. EXPERIMENTAL SETUP AND SAMPLE PREPARATION

The basic technique and experimental setup was essentially the same as for the measurement of germanium, described in the previous paper.⁴ High-energy electrons bombard a biased extrinsic (usually *p*-type) semiconductor and create a thin layer of charge which drifts through the semiconductor. This current "pip" associated with the drifting charge layer is filtered from the equilibrium current, and its duration provides a measure of the transit time of electrons in the sample.

The material used in all experiments was commercially available, high-purity *p*-type InSb, supplied by Cominco and Monsanto. Samples with resistivities ranging from 5 to 280 Ω cm (at 77 °K) have been used. Since the main problem encountered in the measurement is the occurrence of very fast trapping, care has to be taken to remove all damage that can occur during handling of the samples. InSb in particular is susceptible to damage from cold working, and therefore only the center parts of the slices as obtained from the suppliers were retained, and the rest removed with fine abrasive.

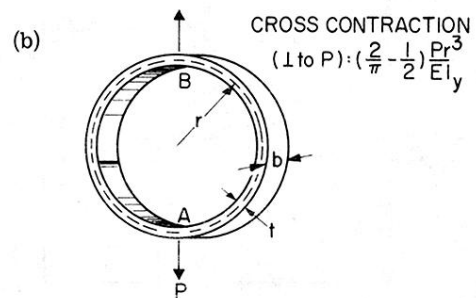
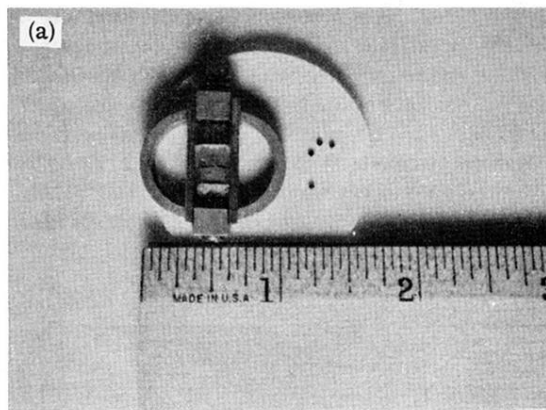


FIG. 5. (a) Photograph of the pressure mechanism.
 (b) Basic spring mechanism.